Fusion Engineering and Design 144 (2019) 148–153

Contents lists available at ScienceDirect

Fusion Engineering and Design

journal homepage: www.elsevier.com/locate/fusengdes

Development of the material property handbook and database of CuCrZr

Kuo Zhang[a,b,*], Ermile Gaganidze[a], Michael Gorley[c]

[a] Karlsruhe Institute of Technology, Institute for Applied Materials, Hermann-von-Helmholtz-Platz 1, 76344, Eggenstein-Leopoldshafen, Germany
[b] Max Planck Institute of Plasma Physics, Boltzmannstraße 2, 85748, Garching, Germany
[c] UK Atomic Energy Authority, Culham Science Center, Abingdon, Oxfordshire, OX14 3DB, UK

ARTICLE INFO

Keywords:
CuCrZr
Material property handbook
EU-DEMO

ABSTRACT

This paper covers the initial progress on the development of material property handbook (MPH) of baseline CuCrZr, within the Materials Engineering Data and Design Integration (MAT-EDDI) of EUROfusion Material Database and Handbook group. Initial drafting of the baseline CuCrZr MPH structure is presented, with inclusion of available data, figures and general information. A data reviewing procedure is discussed for qualification of the data of CuCrZr by comparing raw data from a large variety of resources. If the data scattering is acceptable, average and minimum curves are fitted as suggestions for the European DEMO (EU-DEMO) design. Specific missing properties as well as gaps in the database for EU-DEMO are identified.

1. Introduction

CuCrZr is a precipitation hardening copper alloy. It is characterized by comparatively high strength even at elevated temperatures, high wear resistance and high tempering resistance compared to most copper-based alloys [1,2]. Currently, CuCrZr is the prime candidate heat sink material for high heat flux and plasma-facing components in the EU-DEMO divertor [3]. The lower service temperature limit under irradiation lies between 150°C and 250°C [3]. The recommended upper temperature limit is 350°C for long term operation [4]. The mechanical properties and thermal conductivity of this alloy are some of the key properties of interest in component design for fusion power plant [1].

The purpose of the material property handbook (MPH) on CuCrZr is to provide ready reference and guidance to select the required material properties with engineering trend curves under requirements for design, allowing straightforward use in codes and standards, e.g. Structural Design Criteria (SDC-IC) [5].

To initiate the development of the material database on CuCrZr used for the MPH, literature data has been reviewed and screened. The selected literature was limited for the application in fusion. This paper provides an overview of the literature that has been screened and presents the initial work on the development of the MPH from reviewed literature data.

2. General information

2.1. Chemical composition

The percentage of chemical compositions in the CuCrZr alloy is designated to satisfy the required mechanical and electrical properties.

The content of Cr should be high enough above the solubility limit for the alloy at the solution annealing (SA) temperature to account for Cr inhomogeneity and low enough to prevent coarse Cr precipitates which may cause embrittlement of the alloy. Zr is required for improved homogeneity of precipitates, improved ductility and fatigue resistance. Zr also increases the solubility of Cr in the Cu-Cr-Zr system. P content should be kept as low as possible to minimise coarse precipitates which are stable at SA temperatures of 1050 °C [6,7].

There are various standards defining the chemical composition ranges for the CuCrZr alloy, for instance EN12163 [8] and C18150 [9]. In the ITER Grade CuCrZr (CuCrZr-IG), the weight percentages (wt%) have been specified as Cr: 0.6˜0.9 wt%, Zr:0.07˜0.15 wt% [2]. The other minor alloying elements (Fe, Si, Co, Cd, O) are rarely mentioned in the literature about CuCrZr-IG.

In the MPH of CuCrZr, a table of chemical compositions has been presented, including the specification in various standards and measured values in different reports or product sheets [8–14]. For the

Abbreviation: AT, Arbeitskreis Thermophysik; CTE, Coefficient of Thermal Elongation; DSC, Differential Scanning Calorimetry; ER, Electric Resistivity; EU-DEMO, European DEMO; HT, Heat Treatment; IG, ITER Grade; LCF, Low Cycle Fatigue; LFA, Laser-Flash Apparatus; MPH, Material Property Handbook; PA, #Heat treatment defined in section 1.2; RT, Room Temperature; SA, Solution Annealing; SAA, #Heat treatment defined in section 1.2; SAcwA, #Heat treatment defined in section 1.2; SAoverA, #Heat treatment defined in section 1.2; SCA, #Heat treatment defined in section 1.2; SD, Standard Deviation; SDC-IC, Structural Design Criteria for In-Vessel Components; TC, Thermal Conductivity; UIUC, University of Illinois at Urbana-Champaign, Urbana; UTS, Ultimate Tensile Strength; YS, Yield Strength

* Corresponding author.
E-mail addresses: kuo.zhang@ipp.mpg.de, kuozhang@outlook.com (K. Zhang).

https://doi.org/10.1016/j.fusengdes.2019.04.094
Received 1 February 2019; Received in revised form 24 April 2019; Accepted 29 April 2019
Available online 14 May 2019
0920-3796/

purposes of this paper, only materials meeting the requirements of the ITER grade CuCrZr composition are considered.

2.2. Heat treatment

The properties of CuCrZr alloys are known to be sensitive to heat treatment. Various mechanical properties and also physical properties e.g. electrical/thermal conductivity can be modified with different temperatures and the length of solution annealing and aging times. The cooling rate is also a factor to influence the material properties. For instance, in [11], the yield- and tensile strengths, and also microstructures of specimens with different cooling rates and different aging periods are compared and the highest strength is reported at an aging temperature of 440 °C irrespective of the cooling rate. For the same aging temperature, the strength is increased with the cooling rate but the difference in the strength became smaller when the CuCrZr alloys were aged over 580 °C.

For the application in ITER or EU-DEMO in the future, several heat treatments are specified for CuCrZr, which are listed as a), b), c), d), e) in the following. The most reported heat treatment in literature is SAA, standing for Solution Annealing and Aging. SAcwA includes cold working before aging. SCA includes HIP-treatments. SAoverA means over-aged. And PA stands for Prime Aging.

a) **SAA** – Solution annealing at 980˜1000 °C for 30˜60 min, water quench and age at 460˜500 °C for 2˜4 h. [2,15,16]
b) **SAcwA** – Solution annealing at 980˜1000 °C for 30˜60 min, subsequent cooling in water, further cold working by 40˜70%, and ageing at 450˜470 °C for 2˜4 h. [16]
c) **SCA** – received as SAA, HIP-treated at 1040 °C for 2 h at 140 MPa followed by solution annealing at 980 °C for 0.5 h with a slow cooling rate of 50˜80 °C/min between 980 and 500 °C, and final aging at 560 °C for 2 h. [15]
d) **SAoverA** – Solution annealing and ageing at non-optimal condition (over-aged) due to specific manufacturing processes. [16]
e) **PA** – Reported in a series of papers of B.N. Singh et al. [17–19], material supplied by Outokumpu Oyj (Finland) [20]: solution annealed at 960 °C for 3 h, water quenched and then prime aged (PA) at 460 °C for 3 h.

Although SAA and SAcwA are the two most reported heat treatments, they have never been designated to be the standard heat treatment for CuCrZr, since researches still continue to study the influence of heat treatment/ cold working on the mechanical properties of this alloy, by e.g. modifying the solution annealing temperature or period, cold working degree, aging temperature or period, or by further treatment such as HIP-treatments.

2.3. Content in the MPH of CuCrZr

The material properties have been grouped to mechanical properties and thermo-physical properties in the MPH as follows.

A: Mechanical properties:
A1. Young's modulus
A2. Stress-strain curve
A3. Yield strength
A4. Ultimate tensile strength
A5. Uniform elongation
A6. Total elongation
A7. Hardness
A8. Fatigue
A9. Creep-fatigue
a) Stress-controlled tests
b) Strain-controlled tests
c) Balanced load, extension-controlled
A10. Creep
A11. Fracture toughness
A12. Charpy impact strength
B: Thermo-physical properties:
B1. Coefficient of thermal expansion
B2. Density
B3. Specific heat
B4. Thermal conductivity
B5. Electric resistivity

These properties have been selected for the need to derive the required design curves to match the design requirements, which can explain the performance of the material covering the anticipated failure modes. It also matches with existing properties collected for Eurofer97 [21,22].

Due to the variety of CuCrZr alloys in terms of chemical compositions and heat treatments, even within the ITER Grade, the mechanical and physical properties will differ one from the other. The measured values in various laboratories will be also different from each other due to, for instance, various specimen sizes, accuracy of measurement equipment, loading type and rate, environments (air or vacuum), and so on.

The new MPH of CuCrZr includes all available information and tries to reveal the sensitivity of the material properties to each influencing factor. If the chemical compositions in the reviewed literature are not within the ITER-IG specification, or the temperature and period of solution annealing and aging are not within the five specifications (SAA, SAcwA, SAoverA, SCA, PA) mentioned above,they will be then specially pointed out in the diagrams or text in the MPH.

If the mechanical / physical properties agree well with each other, average curves have been proposed for the CuCrZr alloys to show the relationship between material properties and the testing temperatures. Minimum curves have been also proposed with a distance of 1.96 times the standard deviation (SD), according to ITER Structural Design Criteria for In-Vessel Components (SDC-IC) [5].

To ensure acceptability, the selected literature data have been reassessed aiming at completion of the required information or at judgement of the validity of the collected results according to the international testing standards, e.g. ASTM standards.

Due to a large amount of information in the MPH of CuCrZr, the following part of the current paper will present selectively some important diagrams with discussions from the MPH.

3. Tensile properties

The section on tensile properties includes Young's modulus, stress-strain curves, yield strength (YS) and ultimate tensile strength (UTS), uniform and total elongation.

It is supposed that the reliable data for Young's modulus will be issued from sonic measurements, namely dynamic method. However, until now there is no available report claiming the Young's modulus was measured with this dynamic method. Hence it is supposed that all available Young's modulus of CuCrZr are determined from the tensile stress-strain curves, although it is not everywhere mentioned. Fig. 1 collects the Young's modulus of SAA and SAcwA specimens from several reports. The average and minimum curves are fitted for both SAA and SAcwA specimens.

The equations for fitting curves of Young's modulus are as follows:

$$\textbf{Eaverage, SAA}\,(\mathrm{T})\ -\ \mathrm{GPa} = -1.9234\times10^{-4}\times T^2 - 2.1233\times10^{-2}\times T + 124.91\ (\mathrm{SD}=5.35,\ \mathrm{T}-\ ^\circ\mathrm{C}) \quad (1)$$

$$\textbf{Eaverage, SAcwA}\,(\mathrm{T})\ -\ \mathrm{GPa} = -4.1707\times10^{-5}\times T^2 - 3.3692\times10^{-2}\times T + 129.91\ (\mathrm{SD}=1.81,\ \mathrm{T}-\ ^\circ\mathrm{C}) \quad (2)$$

In order to build analytical or numerical material model, it is more proper to use data from true stress-strain curves. Normally a dog-bone

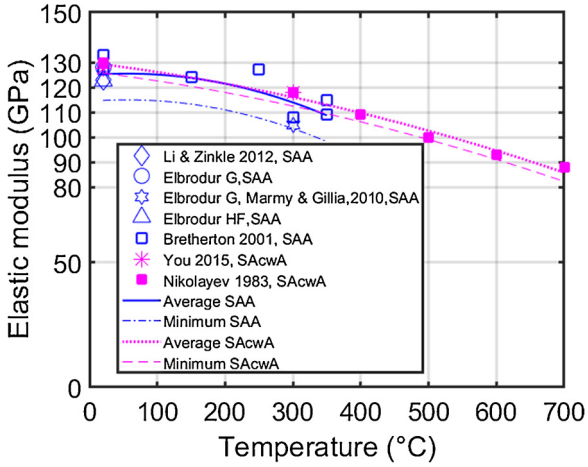

Fig. 1. Young's modulus versus temperatures. [1,7,23–25].

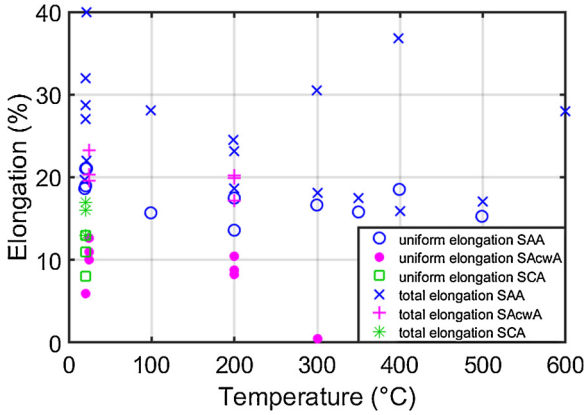

Fig. 3. Uniform and total elongations versus temperatures [1,15,26,30–33].

shaped flat sample should be used together with video record, with which the true stress-strain curve can be calculated. However, such reported result is not yet available today. Hence all the stress-strain curves collected in the MPH of CuCrZr are engineering stress-strain curves.

The stress-strain curves are available at several testing temperatures like room temperature, 150 °C, 200 °C, 250 °C, 300 °C, 400 °C, 500 °C and 600 °C.

The 0.2%-yield strength (YS) and ultimate tensile strength (UTS) in the temperature range 20–700 °C are collected from various reports, as illustrated in Fig. 2. The fitted average curves of yield strengths vs. testing temperatures are quadratic, while linear relationships are revealed between the UTS and the testing temperatures, for both groups of specimens with or without cold working.

The equations for the fitting curves/lines of YS and UTS are as follows:

$$\textbf{YSaverage, SAA}\,(\mathrm{T})\ -\ \mathrm{MPa} = -2.2847\times10^{-4}\times T^2 - 0.13931\times T + 292.19(\ \mathrm{SD} = 24.663,\ \mathrm{T}-\ ^\circ\mathrm{C}) \quad (3)$$

$$\textbf{YSaverage, SAcwA}\,(\mathrm{T})\ -\ \mathrm{MPa} = -4.5936\times10^{-4}\times T^2 - 0.089841\times T + 392.46(\ \mathrm{SD} = 37.84,\ \mathrm{T}-\ ^\circ\mathrm{C}) \quad (4)$$

$$\textbf{UTSaverage, SAA}\,(\mathrm{T})\ -\ \mathrm{MPa} = -0.42631\times T + 413.45(\ \mathrm{SD} = 25.415,\ \mathrm{T}-\ ^\circ\mathrm{C}) \quad (5)$$

$$\textbf{UTSaverage, SAcwA}\,(\mathrm{T}) = -0.4219\times T + 495.4\ \mathrm{SD} = 29.85,\ \mathrm{T}-\ ^\circ\mathrm{C}) \quad (6)$$

When comparing the strengths of different groups of specimens, it is found that cold working increases both the yield and ultimate tensile strengths by approximately 100 MPa. And specimens with HIP-treatments (SCA) have relatively lower yield and ultimate tensile strengths. However the data for SCA specimens are only available at room temperature [15]. More data are required at elevated temperatures to evaluate the effect of HIP-treatments.

The uniform and total elongations are also collected from various reports for the MPH of CuCrZr. The data points are collected in Fig. 3. Comparing to other material properties, the elongation values are relatively rare and scatter too much to propose convincing average curves for the design. In spite of the data scattering, it is obvious that cold working decrease both uniform and total elongation. Note that the HIP-treatments decrease both strength and elongation, while cold working decreases the elongation but increases the strength, as shown in Fig. 2 and Fig. 3.

4. Fatigue and creep

Mechanical properties such as fatigue, creep and creep-fatigue behavior are collected for the MPH of CuCrZr.

To evaluate the influence of testing temperatures on the low cycle fatigue (LCF) behavior, the values which originate from University of Illinois at Urbana-Champaign, Urbana (UIUC) are gathered in Fig. 4. No clear temperature trend is found between data points from room

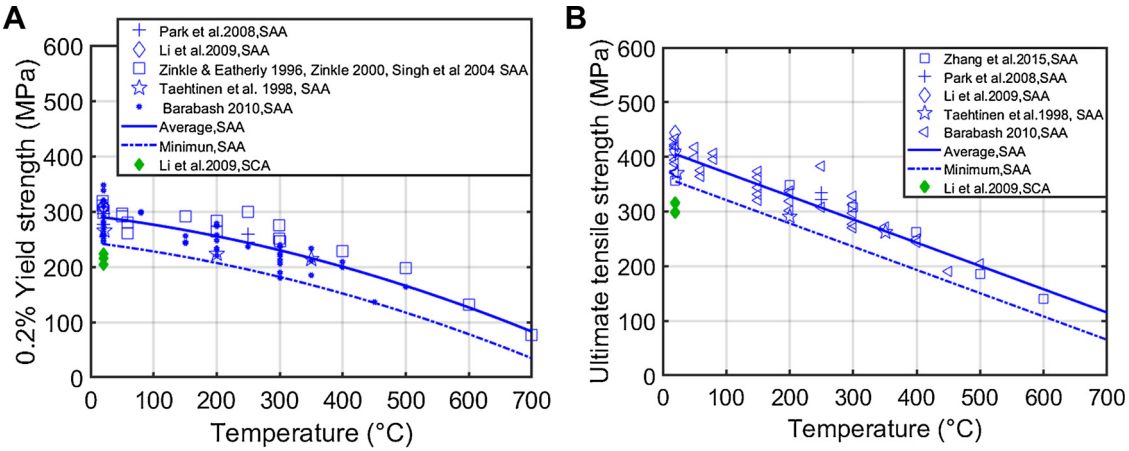

Fig. 2. Yield and ultimate tensile strengths versus temperatures. (a) 0.2%-Yield strengths of SAA and SCA specimens [2,11,15,16,26–29]. (b) 0.2%-Yield strengths of SAcwA specimens [1,2,16,30]. (c) Ultimate tensile strengths of SAA and SCA specimens [11,12,15,16,26]. (d) Ultimate tensile strengths of SAcwA specimens [1,16,30,31].

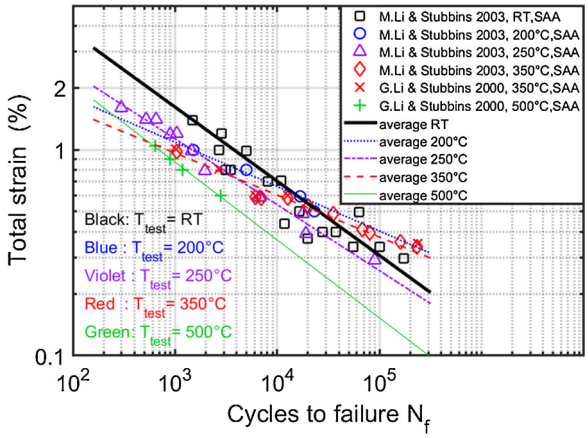

Fig. 4. Total strains versus number of cycles to failure of tests performed in UIUC [34,35].

temperature to 350 °C. Although data points for 500 °C form the lower boundary. Hence, the test temperature (< 500 °C) has marginal influence on the lifetime in LCF tests.

The relationships of total strains versus testing temperatures are shown separately for SAA and SAoverA in Fig. 5. Coffin-Manson fittings are performed for the two groups of data points. The over-aging increases the fatigue life of CuCrZr, which is obvious in the report of Marmy [24]. The specimens have been aged at 580 °C for 2 h, comparing to 460˜500 °C as the aging temperature for SAA specimens.

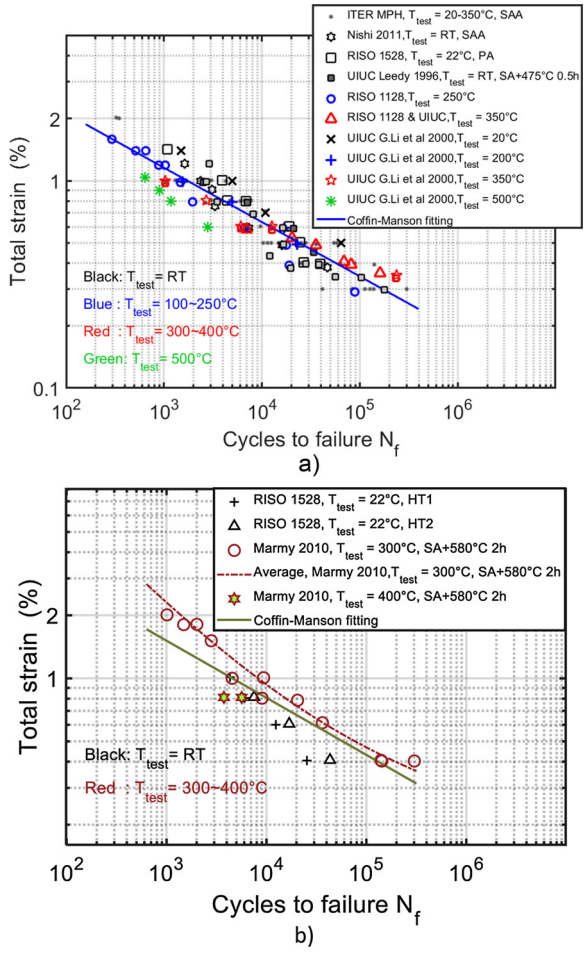

Fig. 5. Total strains versus number of cycles to failure of tests of a) SAA specimens and b) SAoverA specimens [18,24,34–38].

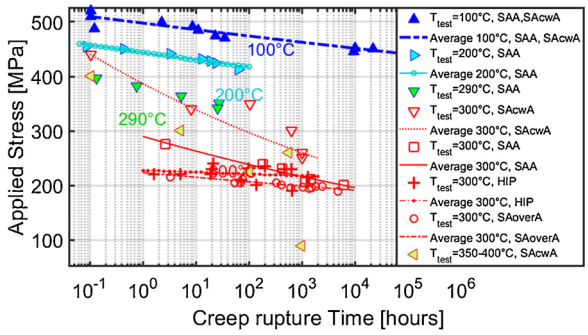

Fig. 6. Creep rupture times versus applied stresses at different testing temperatures. [24,39].

The fitted Coffin-Manson equations for SAA and SAoverA specimen are as follows:

$$\frac{\Delta\varepsilon_{SAA}}{2} = 3.5286 \times N_f^{-0.26199}(\Delta\varepsilon - \%) \quad (7)$$

$$\frac{\Delta\varepsilon_{SAoverA}}{2} = 4.9741 \times N_f^{-0.27269}(\Delta\varepsilon - \%) \quad (8)$$

The proposed Coffin-Manson equation by Marmy [24] for the overaged specimens (aged at 580 °C for 2 h and tested at 300 °C) is as follows:

$$\frac{\Delta\varepsilon_{P.Marmy\ 2010}}{2} = 0.36012 \times N_f^{-0.0812} + 30.968 \times N_f^{-0.50486}(\Delta\varepsilon - \%) \quad (9)$$

The available data for creep is only found in the two reports of Marmy et al. [24,39], which have collected even earlier data points. The data points are summarized in Fig. 6.

Data points for 100 °C match with each other, no matter which heat treatment, cold working or chemical composition there are. Only one group of data exists for 200 °C, which has lower applied stress than those at 100 °C.

The data points for temperatures over 290 °C scatter in a large range. The data from the cold worked alloy form the upper boundary while those from over-aged alloy form the lower boundary. Data points of SAA specimens and those with HIP-treatments lie in between.

For a convincing suggestion to the design, more creep tests are required.

Singh et al. have performed a thorough investigation of creep-fatigue behavior of CuCrZr and reported their results in Risø-R-1528(EN) in 2005 [18]. The material was supplied by Outokumpu Oyj [20] with compositions of Cu - 0.73% Cr – 0.14% Zr, which is within the specified chemical compositions of the ITER Grade CuCrZr. The heat treatments of the specimens include prime aging (PA), which differs itself from traditional SAA by longer solution annealing period (3 h). There have been also other heat treatments in the work of Singh et al. [18], including HT1, HT2. HT1 means PA specimens are further aged in vacuum at 600 °C for one hour. HT2 means PA specimens are further aged in vacuum at 600 °C for four hours.

Singh et al. [18] have performed three groups of creep-fatigue tests: a) stress-controlled, b) strain-controlled, and c) extension-controlled. Since the results have been clearly presented in [18], there is no need to repeat their diagrams in the current paper. Note that Singh et al. [18] have reported ratcheting behavior in the stress-controlled creep-fatigue tests, however without further evaluation. There have been till now no available research on the ratcheting behavior of CuCrZr.

5. Thermo-physical properties

Thermo-physical properties collected for the current MPH of CuCrZr include coefficient of thermal elongation (CTE), density, specific heat, thermal conductivity and electric resistivity.

Pintsuk et al. [40] have reported a thorough investigation on the thermo-physical properties, namely "Interlaboratory tests", where eight European laboratories and a company Netzsch as an external reference laboratory have took part in, to perform thermo-physical tests on specimens from the same batch of material. The material for this "Interlaboratory tests" was taken from a bar material (35 × 35 × 1000mm^3) produced by the company Zollern/Laucherthal [41]. The composition is Cu–0.8Cr–0.08 Zr (in mass%) with low hardness when compared to other CuCrZr grades. Its production process consists of solution annealing at 970 °C for 20 min followed by water quenching and aging at 475 °C for 2 h. The measured data may scatter from each other due to various unknown experimental conditions.

The measurements of coefficient of thermal elongation have been performed with push-rod dilatometry. The majority of the laboratories provided data within a standard deviation of ~3% from the average. Only the results of two laboratories are located outside this range representing the lower threshold (TU-Vienna) and the upper threshold (Netzsch) of the measured CTE data by an offset of ± 5% in comparison to the average. Since there is no reason to exclude either result, both data sets were taken into account and due to its symmetric spread around the average, they balance each other.

The value of density has been measured at room temperature and calculated for T > RT with data of coefficient of thermal expansion.

The specific heats have been measured both by Differential Scanning Calorimetry (DSC) and by Laser-Flash Apparatus (LFA). The specific heats measured on 5 mm thick LFA specimens scatter 2%–4% from the average measured by DSC, while the values measured on 3 mm thick specimen are in very good agreement within the standard deviation of the DSC measurement.

Thermal conductivity (TC) is the most reported thermo-physical property in literature. In the "Interlaboratory tests", the TC has been calculated via the formula

$$\lambda(T) = a(T)\rho(T)cp(T) \tag{10}$$

where λ is thermal conductivity, a is thermal diffusivity, ρ is material density and c_p is specific heat.

For the MPH of CuCrZr, data for TC from more sources are collected. In Fig. 7, the data points and curves are shown.

Fig. 7 shows average thermal conductivity values as well as values from various laboratories in the "Interlaboratory tests". Data points and curves from other sources are also shown in this diagram. Pintsuk et al. [40] have also reported another investigation campaign "Arbeitskreis Thermophysik" (AK), where the thermal conductivity of the same material have been measured. These values from AK are also shown in Fig. 7.

Further, two ITER documents [42,43] are found for the thermal conductivity. These two ITER documents have referred to different sources and have proposed different average curves for the thermal conductivity versus temperature. The difference decreases with increasing temperature. These two curves are also shown in Fig. 7.

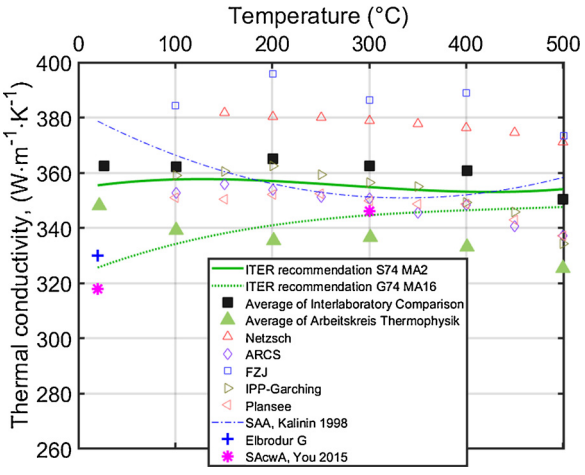

Fig. 7. Thermal conductivities versus temperatures [1,14,29,40,42,43].

The suggested average TC1 by [43] is closer to the results from "Interlaboratory tests", while the suggested average TC2 by [42] is closer to the results from "Arbeitskreis Thermophysik".

Electric resistivity (ER, ρ) can be calculated from thermal conductivity (λ) according to Wiedemann-Franz relation: $\lambda \cdot \rho = L \cdot T$, where T is the absolute temperature and L is the Lorentz number 2.45 × 10^{-8} W·Q·K^{-1}.

6. Gaps in the database

Gaps and non-ideal integration of available data have been discussed respectively for the material properties. Several properties are missing in the database, for instance reduction of area during tensile tests, Poisson's ratio and ratcheting behavior.

Generally, there remains a significant volume of missing data to provide sufficient material properties to enable the full design of EU-DEMO divertor components using CuCrZr. A crucial point is that, the variations of the metallurgical parameters during production procedure have strong influence on the mechanical properties of this material. The specimens from different semi-finished product forms have to be characterized in order to assess the effect of different fabrication procedures (for instance hot radial pressing) on the material properties.

The closing of the database gaps under specified heat treatments should be complemented, including tests after material has been exposed to long term aging conditions mimicking component operation, as well as after dedicated thermo-mechanical treatments simulating the application relevant joining technologies.

To provide convincing design rules, more mechanical tests are expected. For instances, as mentioned in section 3 while discussing the tensile properties of this material, tests are expected to generate the true stress-strain curves at various testing temperatures, to support building of analytical or numerical material models. Besides, more tests for various damage modes are expected, including ratcheting, exhaustion of ductility, fatigue and creep-fatigue [44].

Irradiation campaigns has been launched for CuCrZr upto 5 dpa, irradiation temperatures ranging between 100 °C and 300 °C, for determination of the design relevant mechanical and thermo-physical properties in the irradiated state for base materials and joints. Results including tensile, toughness and LCF properties from post irradiation examination are expected to be available before 2020 [44].

7. Summary

The current paper has reported the early development of EUROfusion material database and material property handbook on ITER-Grade CuCrZr. The database currently includes around 1000 raw material data records taken from literature and screened for acceptability. It is found that the material properties are marginally influenced by factors such as chemical composition, specimen size and loading rates, however are very sensitive to factors including heat treatment and cold working. Various periods and temperatures during solution annealing and aging, as well as various cooling rates, lead to very different material properties. When meaningful, the best estimate trend and minimum curves are proposed for ITER-Grade alloys. Definition of the baseline CuCrZr material and relevant heat treatments will be required in the future, in terms of a) Industrial fabrication of large charge of baseline CuCrZr. b) Characterization campaign for generation of consistent mechanical and thermo-physical data.

Acknowledgements

This Work has been carried out within the framework of the

EUROfusion Consortium and has received funding from the Euratom research and training programme 2014-2018 and 2019-2020 under grant agreement No 633053. M. Gorley would also like to thank the RCUK Energy Programme under grant EP/I501045. The views and options expressed herein do not necessarily reflect those of the European Commission.

References

[1] J.-H. You, Copper matrix composites as heat sink materials for water-cooled divertor target, Nucl. Mater. Energy 5 (2015) 7–18.
[2] V. Barabash, A. Peacock, S. Fabritsiev, G. Kalinin, S. Zinkle, A. Rowcliffe, et al., Materials challenges for ITER – current status and future activities, J. Nucl. Mater. 367-370 (2007) 21–32.
[3] J.H. You, G. Mazzone, E. Visca, C. Bachmann, E. Autissier, T. Barrett, et al., Conceptual design studies for the European DEMO divertor: rationale and first results, Fusion Eng. Des. 109-111 (2016) 1598–1603.
[4] J.-H. You, A review on two previous divertor target concepts for DEMO: mutual impact between structural design requirements and materials performance, Nucl. Fusion 55 (2015) 113026.
[5] ITER Structural Design Criteria for In-Vessel Components (SDCIC), ITER Organization, 2004.
[6] M. Appello, P. Fenici, Solution heat treatment of a Cu-Cr-Zr alloy, Mater. Sci. Eng. A 102 (1988) 69–75.
[7] A.K. Nikolaev, A.I. Novikov, V.M. Rozenberg, Chromium Bronzes, Maetallurgiya, 1983.
[8] Copper and Copper Alloys-Rod for General Purposes, British Standards Institution (BSI), 2011.
[9] Standard Designation for Wrought Copper Alloys, Copper Development Association Inc., 2018.
[10] R. Wei, Q. Li, W.J. Wang, J.C. Wang, X.L. Wang, C.Y. Xie, et al., Microstructure and properties of W-Cu/CuCrZr/316L joint bonded by one-step HIP technique, Fusion Eng. Des. 128 (2018) 47–52.
[11] J.-Y. Park, J.-S. Lee, B.-K. Choi, B.G. Hong, Y.H. Jeong, Effect of cooling rate on mechanical properties of aged ITER-grade CuCrZr, Fusion Eng. Des. 83 (2008) 1503–1507.
[12] X.W. Zhang, X. Zhou, Q.J. Wang, B. Liang, Tensile behavior of high temperature Cu-Cr-Zr alloy, Presented at the International Conference on Power Electronics and Energy Engineering, (2015).
[13] B. Zhang, Z.-g. Zhang, W. Li, Mechanical properties, electrical conductivity and microstructure of CuCrZr alloys treated with thermal stretch process, Trans. Nonferrous Met. Soc. China 25 (2015) 2285–2292.
[14] ELBRODUR Alloys for Resistance Welding, KME Germany GmbH & Co. KG, 2015.
[15] M. Li, M.A. Sokolov, S.J. Zinkle, Tensile and fracture toughness properties of neutron-irradiated CuCrZr, J. Nucl. Mater. 393 (2009) 36–46.
[16] V. Barabash, K. Ioki, M. Merola, G. Sannazzaro, N. Taylor, Materials for the ITER Vacuum Vessel and In-vessel Components- Current Status, (2010).
[17] B.N. Singh, D.J. Edwards, S. Tähtinen, Effect of Heat Treatments on Precipitate Microstructure and Mechanical Properties of CuCrZr Alloy, Risø National Laboratory, 1436 (EN), 2004.
[18] B.N. Singh, M. Li, J.F. Stubbins, B.S. Johansen, Creep-Fatigue Deformation Behaviour of OFHC-Copper and CuCrZr Alloy With Different Heat Treatments and With and Without Neutron Irradiation, Risø-Report, Risø-R-1528(EN), 2005.
[19] B.N. Singh, S. Tähtinen, P. Moilanen, P. Jacquet, J. Dekeyser, D.J. Edwards, et al., Final Report on In-reactor Creep-fatigue Deformation Behaviour of a CuCrZr Alloy: COFAT1, (2007).
[20] Outokumpu. Available: https://www.outokumpu.com/.
[21] E. Gaganidze, F. Gillemot, I. Szenthe, M. Gorley, M. Rieth, E. Diegele, Development of EUROFER97 database and material property handbook, Fusion Eng. Des. 135 (2018) 9–14.
[22] RCC-MRx, Design and Construction Rules for Mechanical Components of Nuclear Installations: High Temperature, Research and Fusion Reactors, (2018).
[23] M. Li, S.J. Zinkle, Physical and Mechanical Properties of Copper and Copper Alloys, Elsevier, 2012.
[24] P. Marmy, O. Gillia, Investigations of the effect of creep fatigue interaction in a Cu-Cr-Zr alloy, Procedia Eng. 2 (2010) 407–416.
[25] L.A. Thi Nguyen, S. Lee, S.J. Noh, S.K. Lee, M.C. Park, W. Shu, et al., Desorption dynamics of deuterium in CuCrZr alloy, J. Nucl. Mater. 496 (2017) 117–123.
[26] S. Tähtinen, M. Pyykkönen, P. Karjalainen-Roikonen, B.N. Singh, P. Toft, Effect of neutron irradiation on fracture toughness behaviour of copper alloys, J. Nucl. Mater. 258-263 (1998) 1010–1014.
[27] S.A. Fabritsiev, S.J. Zinkle, B.N. Singh, Evaluation of copper alloys for fusion reactor divertor and first wall components, J. Nucl. Mater. 233-237 (1996) 127–137.
[28] B.N. Singh, D.J. Edwards, S. Tähtinen, Effect of Heat Treatments on Precipitate Microstructure and Mechanical Properties of CuCrZr Alloy, Risø-R-1436(EN), 2004.
[29] G. Kalinin, R. Matera, Comparative analysis of copper alloys for the heat sink of plasma facing components in ITER, J. Nucl. Mater. 258-263 (1998) 345–350.
[30] G.M. Kalinin, A.S. Artyugin, M.V. Yvseev, V.V. Shushlebin, L.P. Sinelnikov, Y.S. Strebkov, The effect of irradiation on tensile properties and fracture toughness of CuCrZr and CuCrNiSi alloys, J. Nucl. Mater. 417 (2011) 908–911.
[31] G. Kalinin, V. Barabash, A. Cardella, J. Dietz, K. Ioki, R. Matera, et al., Assessment and selection of materials for ITER in-vessel components, J. Nucl. Mater. 283-287 (2000) 10–19.
[32] B.N. Singh, D.J. Edwards, P. Toft, Effects of neutron irradiation on mechanical properties and microstructures of dispersion and precipitation hardened copper alloys, J. Nucl. Mater. 238 (1996) 244–259.
[33] S.A. Fabritsiev, A.S. Pokrovsky, D.J. Edwards, S.J. Zinkle, The effect of neutron dose, irradiation and testing temperature on mechanical properties of copper alloys, J. Nucl. Mater. 258-263 (1998) 1015–1021.
[34] M. Li, J.F. Stubbins, Evaluation of irradiation effect on fatigue performance of copper alloys for high heat flux applications, Fusion Sci. Technol. 44 (2003) 186–190.
[35] G. Li, B.G. Thomas, J.F. Stubbins, Modeling creep and fatigue of copper alloys, Metall. Mater. Trans. A 31A (2000) 2491–2502.
[36] H. Nishi, M. Enoeda, Effect of HIP temperature on microstructure and low cycle fatigue strength of CuCrZr alloy, J. Nucl. Mater. 417 (2011) 920–923.
[37] P. Marmy, In-beam mechanical testing of CuCrZr, J. Nucl. Mater. 329-333 (2004) 188–192.
[38] K.D. Leedy, J.F. Stubbins, B.N. Singh, F.A. Garner, Fatigue behavior of copper and selected copper alloys for high heat flux applications, J. Nucl. Mater. 233-237 (1996) 547–552.
[39] P. Marmy, Creep-Fatigue of Cu-Cr-Zr: a Review of the Existing Fatigue, Creep and Creep-fatigue Data Base and a Life Prediction Analysis Using a Time Based Damage Evaluation, (2005).
[40] G. Pintsuk, J. Blumm, W. Hohenauer, R.C. Hula, T. Koppitz, S. Lindig, et al., Interlaboratory test on thermophysical properties of the ITER grade heat sink material copper–Chromium–Zirconium, Int. J. Thermophys. 31 (2010) 2147–2158.
[41] ZOLLERN. Available: https://www.zollern.com.
[42] ITER Document No. G74 MA16, ITER Material Properties Handbook, File Code: ITER-AK02-3112.
[43] ITER Document No. S74 MA2, ITER Material Properties Handbook, File code : ITER-AK02-3112.
[44] G. Pintsuk, E. Diegele, S.L. Dudarev, M. Gorley, J. Henry, J. Reiser, et al., European materials development: results and perspective, Fusion Eng. Des. (2019), https://doi.org/10.1016/j.fusengdes.2019.02.063.